AFRL-RQ-WP-TP-2013-0058

DIAGNOSTICS FOR HYPERSONIC ENGINE CONTROL

Michael S. Brown and Jeffrey M. Donbar

Hypersonic Sciences Branch
High Speed Systems Division

FEBRUARY 2013

Approved for public release; distribution unlimited.

See additional restrictions described on inside pages

STINFO COPY

AIR FORCE RESEARCH LABORATORY
AEROSPACE SYSTEMS DIRECTORATE
WRIGHT-PATTERSON AIR FORCE BASE, OH 45433-7542
AIR FORCE MATERIEL COMMAND
UNITED STATES AIR FORCE

REPORT DOCUMENTATION PAGE

Form Approved
OMB No. 0704-0188

1. REPORT DATE *(DD-MM-YY)*	2. REPORT TYPE	3. DATES COVERED *(From - To)*
February 2013	Technical Paper	01 March 2011 – 26 February 2013

4. TITLE AND SUBTITLE
DIAGNOSTICS FOR HYPERSONIC ENGINE CONTROL

5a. CONTRACT NUMBER
In-house

5b. GRANT NUMBER

5c. PROGRAM ELEMENT NUMBER
62201F

6. AUTHOR(S)
Michael S. Brown and Jeffrey M. Donbar

5d. PROJECT NUMBER
2404

5e. TASK NUMBER
N/A

5f. WORK UNIT NUMBER
Q039

7. PERFORMING ORGANIZATION NAME(S) AND ADDRESS(ES)
Hypersonic Sciences Branch (AFRL/RQHF)
High Speed Systems Division
Air Force Research Laboratory, Aerospace Systems Directorate
Wright-Patterson Air Force Base, OH 45433-7542
Air Force Materiel Command, United States Air Force

8. PERFORMING ORGANIZATION REPORT NUMBER
AFRL-RQ-WP-TP-2013-0058

9. SPONSORING/MONITORING AGENCY NAME(S) AND ADDRESS(ES)
Air Force Research Laboratory
Aerospace Systems Directorate
Wright-Patterson Air Force Base, OH 45433-7542
Air Force Materiel Command
United States Air Force

10. SPONSORING/MONITORING AGENCY ACRONYM(S)
AFRL/RQHF

11. SPONSORING/MONITORING AGENCY REPORT NUMBER(S)
AFRL-RQ-WP-TP-2013-0058

12. DISTRIBUTION/AVAILABILITY STATEMENT
Approved for public release; distribution unlimited.

13. SUPPLEMENTARY NOTES
PA Case Number: 88ABW-2013-0939; Clearance Date: 26 February 2013. This technical paper contains color.

14. ABSTRACT
The overall goal of the research is to find diagnostic measurements that reliably indicate changes in the dynamics of hypersonic flow paths – scramjet engines in particular. Of primary interest are measurements that serve to indicate that gross changes in flow behavior are about to happen. A priori it is not known if such measurements exist. Local values of state variables (temperature, pressure, velocity, etc.) will necessarily follow changes. The question is whether or not some particular combination of state variables or an additional measureable quantity or quantities can serve as a precursor of impending dynamic changes. Most interesting for hypersonic engine control are changes in isolator margin, inlet mass capture, and performance (thrust, combustion efficiency, etc.).

15. SUBJECT TERMS
diagnostics, boundary layer, scramjets, isolator

16. SECURITY CLASSIFICATION OF: a. REPORT	b. ABSTRACT	c. THIS PAGE	17. LIMITATION OF ABSTRACT:	18. NUMBER OF PAGES	19a. NAME OF RESPONSIBLE PERSON (Monitor)
Unclassified	Unclassified	Unclassified	SAR	18	Jeffrey M. Donbar **19b. TELEPHONE NUMBER** *(Include Area Code)* N/A

Research Objectives:

The overall goal of the research is to find diagnostic measurements that reliably indicate changes in the dynamics of hypersonic flow paths – scramjet engines in particular. Of primary interest are measurements that serve to indicate that gross changes in flow behavior are about to happen. A priori it is not known if such measurements exist. Local values of state variables (temperature, pressure, velocity, etc.) will necessarily follow changes. The question is whether or not some particular combination of state variables or an additional measureable quantity(ies) can serve as a precursor of impending dynamic changes. Most interesting for hypersonic engine control are changes in isolator margin, inlet mass capture, and performance (thrust, combustion efficiency, etc.) To meet this goal we have pursued the following research objectives:

- Determine if an upstream propagating "signal" can be found in the subsonic portion of the boundary layer that precedes gross changes in isolator margin.
- Identify measureable quantities other than thermodynamic state variables that indicate changes in flow dynamics prior to state variable changes.
- Assess the ability of in-stream optical measurements along a few lines of sight at both the isolator entrance and combustor exit to follow changes in flow and heat release and accurately identify the engine state.

Technical Summary:

The scientific literature reflects a lot of careful work by numerous researchers in addressing the receptivity of boundary layers to perturbations. Essentially all of this work dealt with situations in which the perturbation co-propagated with the flow. In a very few instances, researchers in quiet tunnels have noted that disturbances can travel upstream in the subsonic region of laminar boundary layers. We are addressing the question of whether or not similar disturbance propagation can occur in separating and/or turbulent boundary layers. Most importantly from the perspective of flowpath control is whether or not such "signal" propagation might precede a gross change in flow dynamics. For example, a fundamental question regarding a hypersonic combusting flow is whether or not a transient in heat release (that eventually pushes the attendant shock train farther forward in the isolator) manifests itself as a disturbance propagating upstream in the boundary layer ahead of the movement of the shock train.

To address the above fundamental question of upstream propagation of disturbances we conducted two optical experiments in a non-reacting Mach 2 flow. The measurements were made in a rectangular-cross-section constant-area duct. Low-power, continuous-wave (cw), diode-laser beams (0.5 mW, 1.4 μm) were directed span-wise across the floor of the duct just above the floor surface so as to completely lie within the boundary layer. (Previous research had shown the boundary layer momentum thickness in this flow to be about 5 mm. The laser beam diameter was <2 mm.) A controlled downstream disturbance was generated in two ways. First, a pulsed, frequency-doubled, Nd:YAG laser (1.5 J/pulse, 532 nm) was focused into the core flow above the boundary layer about 30 mm downstream of the cw beams. The focused pulsed energy generated a consistent repetitive laser spark with an accompanying cylindrical shock wave at 10 Hz. Upstream, at the location of the cw beams, the passage of the shock-driven disturbance was detected as a momentary transient loss in beam transmission due to aero-optic beam steering. The time-resolved transient transmission loss showed a sharp leading edge (<1 ms) with a recovery time on the order of 5-6 ms. Our working explanation for this observation is that the cylindrical shock wave emanating from the spark impinges on the boundary layer downstream of the spark and disturbs it in such a way that a small pressure wave propagates upstream in the subsonic region of the boundary layer. This wave then leads to the transient in the optical transmission signal.

In the second experiment, the cw diode laser beams were again placed span-wise within the boundary layer just upstream of an injection port oriented normally to the duct floor. The port was fed with the effluent from a small pulse detonation device. Repetitive firing of the detonation device introduced transient plumes of injected hot gases into the core flow. The complex fluid dynamics led to a transient disturbance of the boundary layer that propagated upstream. Similar to the original experiment, the time-resolved transmission of the diagnostic cw beams was affected by this behavior. The affect was more subtle and detection was achieved by monitoring the derivative of the intensity fluctuations in the transmitted beam. In both experiments a 100% correlation was achieved between the disturbing event and the transient beam transmission behavior. These observations naturally lead to many questions regarding the characteristics of the disturbance (energy deposited, frequency spectrum of disturbance, damping distance, etc.) that yield detection upstream in the boundary layer and whether or not these manufactured disturbances are commensurate with those that would occur due to dynamic heat release in a combustor.

Observation of the transients in the proof-of-concept experiments led us to look for similar transients in an axisymmetric flow-path using optical lines of sight that lie in the axial symmetry plane. As such, the beams pass through the boundary layer (on both sides) as well as the core flow. Experiments were conducted in the isolator of a model scramjet engine operated in direct-connect mode. Two cw diode laser beams weredirected across the flow at the entrance to the isolator just downstream of the facility nozzle. The near-infrared beams were frequency tuned across water absorption features such that both a resonant and non-resonant transmission signal could be recorded at a rate of 1 kHz. The resonant part of the signal was post-processed to extract temperature and velocity while the non-resonant portion was examined for fluctuations indicating transient beam steering. Data was collected over various engine operation conditions in which transients were introduced into the isolator via changes in fuel schedule or mass injection. A series of high-frequency pressure transducers located at evenly spaced axial locations between the combustor cavity and the facility nozzle were used to study the dynamics of the shock train structure during these transient combustor events. They revealed the propagation speed of the gross shock movement to be on the order of a few percent of the axial core velocity.

Analysis of the optical data was done in various ways. First the resonant absorption signal was analyzed to yield the time-dependent temperature. Second the rms fluctuations in the intensity of the non-resonant signal were determined as a function of time. Time series histories of these two quantities and their derivatives (with respect to time) were analyzed. By plotting the temperature as a function of time delay, $T(t+\delta t)$, versus the temperature at time t, T(t), for particular fixed values of the delay we find that the data lie in groupings. A specific example is shown in Fig. 1. What is noticeable is that during the transition period between the before and after thermodynamic states, the

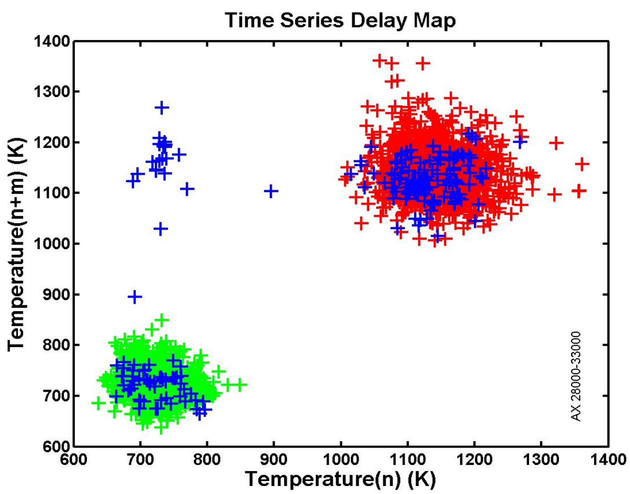

Figure 1. Time-delayed temperature plotted against the non-delayed values before (green), during (blue), and after (red) a transient event that placed the isolator shock train leading edge in the vicinity of the laser beam paths.

locus of points moves from the green to the red through the blue. The implication is that monitoring for points in the time series delay map that lie in the blue provides a precursor signal to a gross fluid behavior. For another engine test, the first and second derivatives of the rms deviations of the non-resonant signal begin to change before the derivatives of the state variable (temperature) change (see Fig. 2). This may reflect dynamic changes in the boundary layer that precede those in the core flow.

The intrinsic density/entropy fluctuations in supersonic boundary layers can be quite short in time – on the order of tens of microseconds. We therefore sought data acquired at higher rates than that just discussed. A separate two-input channel DAQ was implemented for data collection during one run night. This DAQ recorded the photodetector signals at a rate of 100 MHz while two diode lasers were swept (frequency-tuned) repetitively at 10 kHz. Due to some limitations with this hardware, the data collection was done asynchronously with respect to the usual run data set. Consequently we chose to acquire optical transmission signals in the isolator at set engine conditions and look for “fingerprints.”

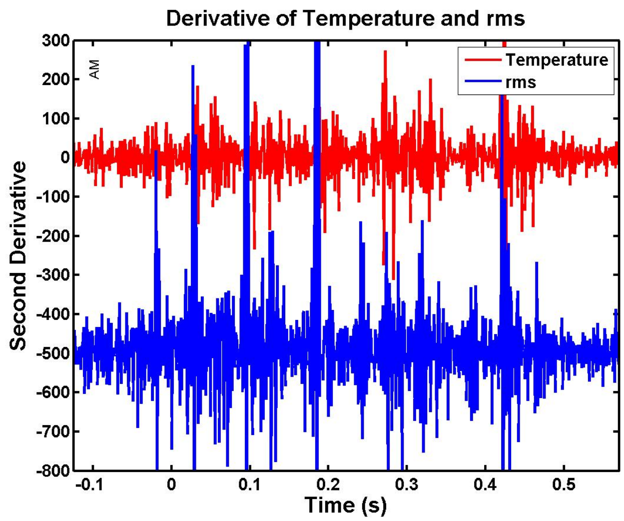

Figure 2. Second order time derivative of the optically-determined temperature and the rms of the non-resonant signal intensity fluctuations acquired during a transient event. The change in the amplitude of the derivative of the rms fluctuations precedes that of the temperature.

Primarily, the nonresonant portions of the transmission signal were examined using the time-lag maps and derivative methods noted above along with the autocorrelation of the signal. The nonresonant signals were processed by first removing the mean. The resulting fluctuations about "zero" were averaged to obtain root-mean-squared (rms) values (and concomitant standard deviations). Numerical first, second, third, and fourth derivatives were calculated along with the autocorrelation. The autocorrelations displayed a similar shape for each engine state. It peaks for zero time delay and then smoothly decays to negative values; reaches a minimum and then rises to a steady-state level. As the engine state changes the 1/e time, and the first zero crossing and minimum signal times change. In Table 1 we report these characteristic times as well as the rms mean and standard deviation of the signal.

In the table, numerical entries appear for six engine states at Mach 4 flight enthalpies. The data was collected in the optical calibrator just downstream of the facility nozzle. The autocorrelation function consistently showed a single negative minimum (anti-correlation) which is displayed in the table along with the 1/e and first zero crossing times. Each column denotes a separate engine state – ten diode laser sweeps were averaged together. For those columns labeled "avg," each of the sweeps in the sequence was itself an average of ten serial recordings of the photodetector signals. The first column indicates values for the relatively quiescent flowpath – the exhausters are on but the vitiator is not. It exhibits the lowest rms fluctuations in the transmitted signal.

Table 1. Measured values of the optical transmission fluctuations. Observed characteristics of the processed transmission signal fluctuations are shown for six engine operating states.

			fueled	fueled	fueled	fueled
Engine State / Signal Feature	no vitiator	vitiator only	high margin	low margin	high margin	low margin
	avg	avg	avg	avg	no avg	no avg
rms mean X 100	0.12	0.27	0.28	0.22	0.43	0.70
std X 100	0.13	0.29	0.28	0.18	0.47	0.72
1/e time of autocorrelation(sec)	1.15	1.20	0.97	2.43	0.39	1.81
1st zero crossing of autocorrelation (sec)	3.22	2.92	2.67	6.33	2.58	6.55
minimum location of autorcorrelation(sec)	6.11	6.41	6.86	8.88	4.77	9.12

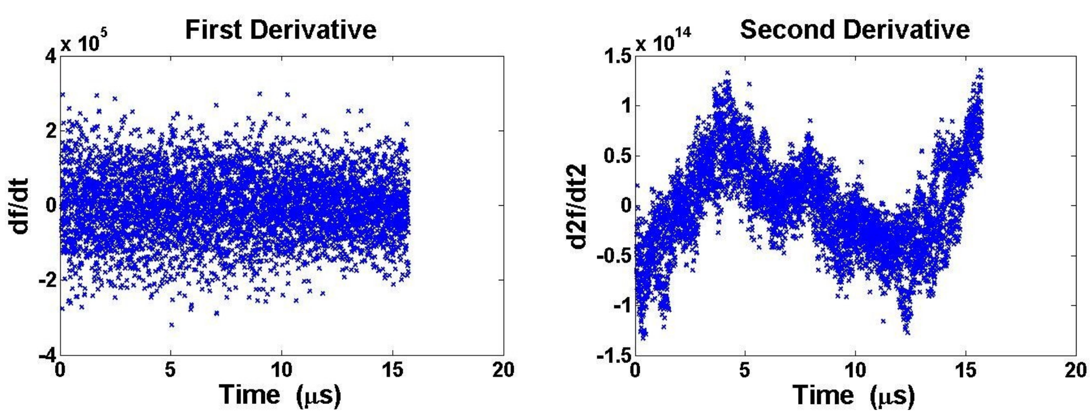

Figure 3. First and second derivatives of transmission fluctuation for engine state corresponding to the low-margin fueled engine state of Table 2.

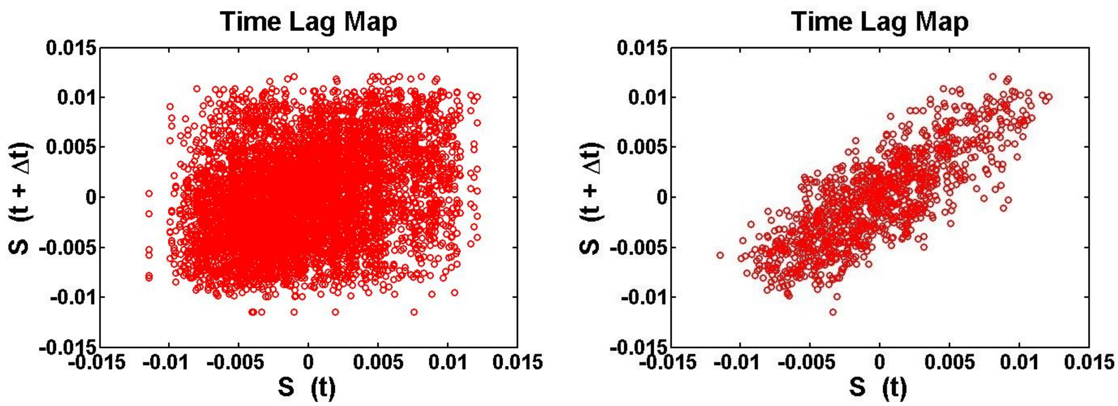

Figure 4. Time-lag maps for high margin engine state; top – 0.1 μs; bottom – 2.0 μs.

The autocorrelation function consistently showed a single negative minimum (anti-correlation) which is displayed in the table along with the 1/e and first zero crossing times. Each column denotes a separate engine state – ten diode laser sweeps were averaged together. For those columns labeled "avg," each of the sweeps in the sequence was itself an average of ten serial recordings of the photodetector signals. The first column indicates values for the relatively quiescent flowpath – the exhausters are on but the vitiator is not. It exhibits the lowest rms fluctuations in the transmitted signal.

High and low margin labels on the columns in this table refer to the relative location of the leading edge of the shock train within the isolator. Low margin means the shock train leading edge is located upstream near the facility nozzle. Attention should be paid to the last two columns which cover two fueled engine states with low and high margins and minimal signal averaging. There is a marked contrast between the two cases. The low margin state exhibits a greater rms fluctuation in the transmission signal and equally interesting the autocorrelation signal shows increased correlation in the form of a longer 1/e correlation time and a greater delay in the first zero crossing and location of the minimum. This indicates local fluid behavior with more "structure" in time than its high-margin counterpart. This could be explained by the presence of larger physical structures in the boundary layer of the low margin case.

Examination of the numerical derivatives (with respect to time) of the transmission fluctuations indicate no structure in the first, third, and fourth derivatives. However, the second derivative typically shows a cubic structure regardless of engine state. In Figure 3 we show an example for the low margin fueled engine state with averaging (column 5 of Table 2).

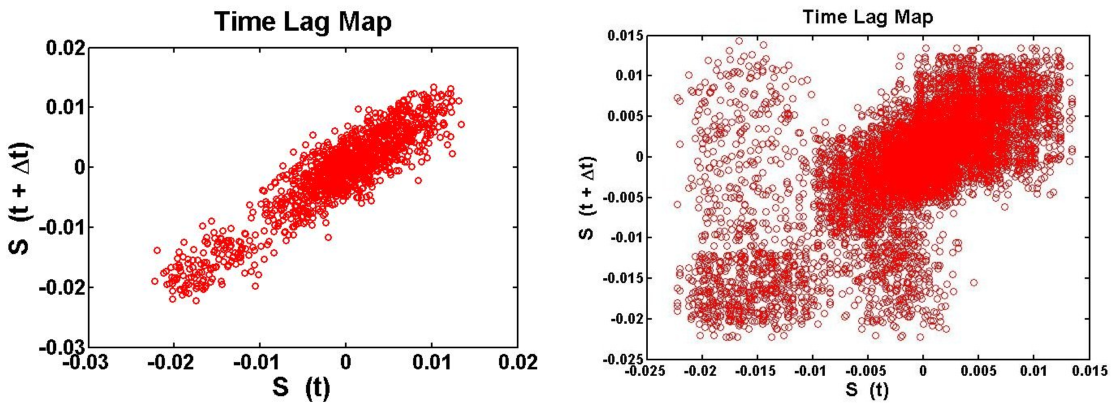

Figure 5. Time-lag maps for low margin engine state; top – 0.1 μs; bottom – 2.0 μs.

Time-lag maps of the transmission intensity fluctuations differ markedly between high-margin and low-margin engine states. In two figures we show examples of time-lag m aps for delays of 0.1 and 2 microseconds. Figure 4 shows the maps for an engine state with high isolator margin. At short time delays (top frame; delay = 0.1 μs) the plot appears linear as there is still high correlation between the signal and its delayed counterpart. In the bottom plot a long delay of 2 μs reveals the absence of correlation or any other higher order structure. The individual points lie in a symmetric cluster that simply spans the range of individual amplitude values for the fluctuation signal.

The situation is very different for an engine state of low isolator margin as the time lag maps of Figure 5 reveal. For short time delays the map looks somewhat similar to that of the high margin case though there clearly are two regions of point concentrations. For long delays, the simple circular symmetry of the high margin case displayed in the bottom half of Figure 4 is replaced by a much more complex structure with two orthogonal planes of symmetry. Again, this points to a more complex fluidic structure in the low-margin case.

Examination of the non-resonant transmission signals acquired in the rotating housing downstream of the combustor reveals a very different picture than that just described for the signals acquired just downstream of the facility nozzle. Both the autocorrelation and derivatives (first – fourth order) indicate no lasting "structure." Likewise, the time-lag maps of the signal are essentially featureless like those in the bottom half of Fig. 4. The 1/e times of the autocorrelation are consistently more than an order of magnitude shorter than those associated with the upstream data under the same engine state. Equally interesting, the rms amplitude of the non-resonant transmission fluctuations is consistently about an order of magnitude larger than that seen in the upstream data. This may simply reflect the density fluctuations introduced into the edges of the core flow from the shear layer that would form between the core flow and the room air that is drawn in between the outer surface of the combustor and the rotating housing.

An alternative method of looking at transient signal intensity fluctuations to find harbingers of gross fluid state changes is shown graphically in Figure 6. In short, we

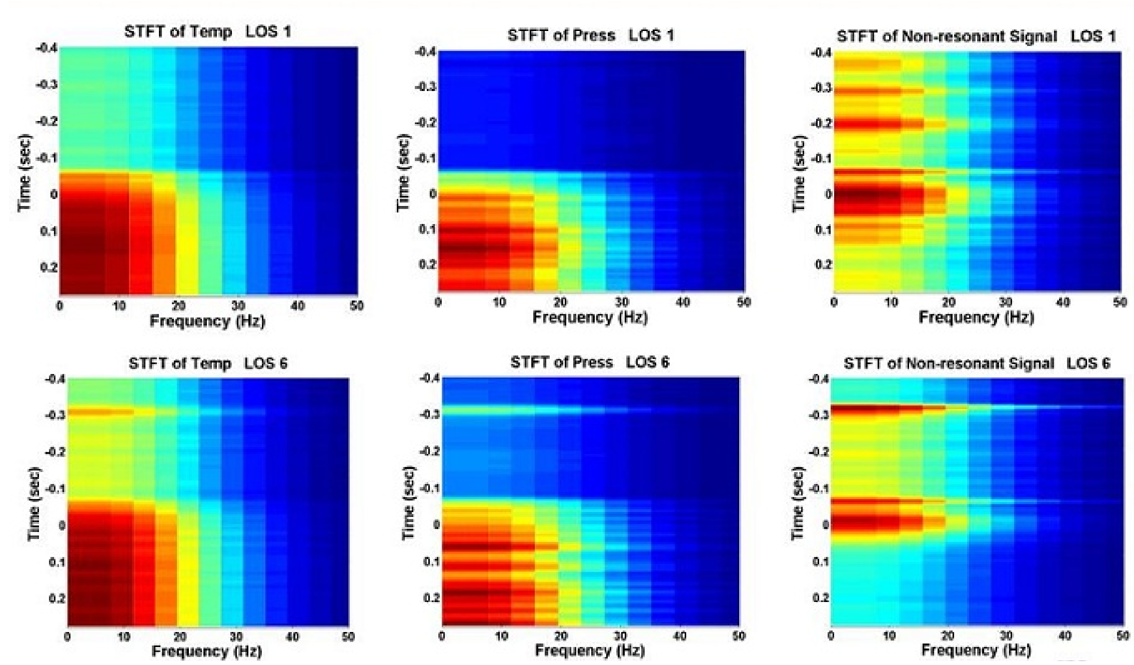

Figure 6. Power spectra derived from short-time (sliding) Fourier transforms of the optically derived values of the local static temperature (column 1), static pressure (column 2), and non-resonant beam deflection signal (column 3). Power spectra are shown for two locations within the isolator of an axisymmetric engine; upstream of combustor (row 1) and near combustor entrance (row 2).

examined the short-time (sliding) Fourier transforms of the time series values for static temperature, static pressure, and beam deflection at two locations within the isolator of a fueled axisymmetric engine. The top row shows the power spectra derived from the Fourier transforms at an isolator location upstream of the combustor while the second row shows the same for a measurement location close to the combustor entrance. The temperature and pressure values were derived from optical absorption measurements. The displayed spectra show content at low frequencies (0-50 Hz) along the x axis for a period of time beginning 0.4 seconds before combustor ignition and 0.3 seconds after ignition (y axis). Time zero indicates ignition. All six plots show significant spectral amplitude from 0 to 20+ Hz at time zero and beyond. For the measurement location closest to the combustor entrance (second row), the temperature, pressure and beam deflection signals all show non-zero content 0.3 sec prior to ignition. Most interestingly, the non-resonant beam deflection signal acquired at the upstream location (first row) shows significant spectral content beginning 0.4 sec before ignition.

While these results are not quantifiably conclusive, the information revealed in Figures 1 through 6 indicates that optical signals may be useful in identifying relative engine states; and, more importantly a changing engine state. It is our current working hypotheses that the boundary layer contains the dynamic information we seek to identify and "predict" engine state changes. This has prompted us to do launch to new lines of research. First, we have designed an experiment to be implemented in a rectangular cross-section flow path operated in Mach 2 non-reacting flow mode. The experiment will use off-the-shelf microphones as sound sources mounted flush with the bottom wall of the flowpath. These sound sources will be located at a downstream location. At various upstream locations we will look for evidence of the propagation of the launched acoustic waves using optical methods (most notably beam deflectometry) along with acoustic methods (microphones) and surface measurements (kulites for local pressure). The underlying premise is that the acoustic signal that propagates upstream in the subsonic portion of the boundary layer should reflect the boundary layer state. If the boundary layer changes due to downstream changes in back pressure the amplitude and bandwidth of the driven acoustic signal is likely to change.

The second avenue of new research was captured in our new LRIR proposal. In brief we will adopt optical imaging techniques developed primarily in the medical community to the close study of boundary layer dynamics. Our technique adaptation is designed to image and identify coherent density structures in boundary layers and look for those indicative of changing boundary layer dynamics.

It is highly desirable to the Air Force to have control of hypersonic flow-paths for both ground testing and flight experiments. The flight work presents additional challenges. In-flight optical measurements will necessarily be more restricted than those discussed above both in terms of hardware limitations (e.g. fewer lines of sight) and the ability to repeat experiments. Consequently, a portion of our research is aimed at learning what level of measurement sophistication is required to unambiguously derive information about the hypersonic flow; and, in the long run provide sensor feedback to engine control strategies. Over the past year experimental work was done using the in-house research facilities and the arc-heated facility at NASA Langley for a few months. Additionally, during the summer of 2011, academic partners executed a computational component to the overall effort. Much of the experimental and computational activities directly feed information/experience to the HIFiRE program – flight 2 in particular. The work is broad enough however to be applicable to future experimental flight activities. Specifically, water-based diode laser absorption measurements were made at the exit plane of the HIFiRE-2 engine being tested at Langley. The flight research goal (with respect to the optical instrumentation) is to assess combustion efficiency by using the absorption spectra to assess the time-dependent temperature, pressure and water density and compare this with calculated combustion efficiency based on known fueling conditions, and wall-pressure measurements combined with low order models as well as CFD. A combustion efficiency sensor could provide feedback to a control system devised to optimize engine performance. Measurements were made at three simulated flight Mach numbers under varying fuel schedule. This data is now being analyzed.

It is well known that inlet flow distortion can greatly alter hypersonic engine performance. While such distortion can be measured using intrusive means such as pitot rakes it would be highly desirable to have non-intrusive capability again with an idea toward development of a sensor for engine control. Line-of-sight absorption measurements are capable of extracting velocity as well as pressure and temperature. The research questions rest with issues such as how many lines of sight are needed to uniquely characterize the distorted (or undistorted flow) and at what axial flow locations should they be placed. Due to time and cost constraints it is not feasible to make enough actual measurements to address all unknowns. So, we sought a computational tool to assist with this aspect of the research. To this end, our academic partners worked with us to develop a FORTRAN code that would make virtual absorption measurements along any specified line of sight(s) through any CFD (or other numerical) solution. As a first test case we have applied the code to CFD solutions executed for HIFiRE Flight 1 post flight. This flight experiment included an optical instrumentation package designed to measure velocity using O_2-based absorption in two cut-outs in the flare at the aft end of the payload. The flow through the cut-outs is quite complex as revealed by the CFD solutions. The optical measurements were studied for a particular time in the vehicle ascent with companion CFD work. The measured velocity and the virtual velocity agree to within uncertainties – both indicating a path-integrated velocity well below that of the axial velocity of the vehicle.

During 2012, this FORTRAN analysis package was transferred from the academic partners to AFRL. Drs. Brown and Hagenmaier have begun using this computational tool set to decide how many optical lines of sight will be needed to acquire needed information during the MSSC engine testing that will commence in 2014 at AEDC. Optical measurements will be used in this effort to assess the level of flow distortion at the entrance to the isolator and to evaluate combustion efficiency at the exit plane of the combustor.

Publications:

J. Liu, and M. S. Brown, "Radiative Heating in Hydrocarbon-fueled Scramjet Engines," AIAA Paper No. 2012-3775, 48th AIAA/ASME/SAE/ASEE Joint Propulsion Conference and Exhibit, Atlanta, GA (30 July - 01 August 2012).

A. J. Crow, I. D. Boyd, M. S. Brown, and J. Liu, "Thermal Radiative Analysis of the HIFiRE-2 Scramjet Engine," AIAA Paper No. 2012-2751, 43rd AIAA Thermophysics Conference, New Orleans, LA (25 - 28 June 2012).

K-C. Lin, C. Carter, M. Brown, S. Smith, and A. Kastengren, "Investigation of Near-Field Structures of Aerated-Liquid Jets Using X-Ray Radiography," ILASS-Americas Paper 2012-027, 24th Annual Conference on Liquid Atomization and Spray Systems, San Antonio, TX (20 - 23 May, 2012).

M. S. Brown, G. C. Herring, K. Cabell, N. Hass, T. Barhorst, and M., Gruber, "Optical Measurements at the Combustor Exit of the HIFiRE 2 Ground Test Engine," AIAA Paper No. 2012-0857, 50th AIAA Aerospace Sciences Meeting, Nashville, TN (9-12 January 2012).

(invited) M. S. Brown, "Application of Diode-Laser-Based Measurements in Hypersonic Flows," AIAA Paper No. 2012-0555, 50th AIAA Aerospace Sciences Meeting, Nashville, TN (9-12 January 2012).

J. M. Donbar, M. S. Brown G. J. Linn, and K-Y. Hsu, "Simultaneous High-Frequency Pressure and TDLAS Measurements in a Small-Scale Axisymmetric Isolator with Bleed," AIAA Paper No. 2012-0331, 50th AIAA Aerospace Sciences Meeting, Nashville, TN (9-12 January 2012).

R. Yentsch and M. S. Brown, *TDLAS Explorer: A Computational Framework for Tunable Diode Laser Absorption Spectroscopy Simulation*, 7th Annual Dayton Engineering Sciences Symposium, Oct. 24, 2011, Dayton, OH.

M. S. Brown and T. Barhorst, “Post-Flight Analysis of the Diode-Laser-Based Mass Capture Experiment Onboard HIFiRE Flight 1,” AIAA Paper No. 2011-2359, 17th AIAA International Space Planes and Hypersonic Systems and Technologies Conference, San Francisco, California, Apr. 11-14, 2011

M. S. Brown, T. Barhorst, D. L. Barone, and W. Terry, “Tomographic Reconstruction of the Temperature and Water Mole Fraction Fields at the Exit of a Scramjet Using TDLAS,” JANNAF 44th Combustion, 32nd Airbreathing Propulsion, 25th Propulsion Systems Hazards Joint Subcommittee Meeting, Arlington, VA (18-21 April 2011).

M. S. Brown, T. Barhorst, M. Gruber, and W. Terry, “Optical Sensor for HIFiRE Flight 2 Scramjet Ground and Flight Experiments,” 36th Annual Dayton-Cincinnati Aerospace Sciences Symposium, Dayton, OH (1 March 2011).

R. J. Yentsch, D. Gaitonde, and M. S. Brown, “CFD Simulations of HIFiRE Flow Fields,” 36th Annual Dayton-Cincinnati Aerospace Sciences Symposium, Dayton, OH (1 March 2011).